New Phytologist / Volume 212, Issue 1 / p. 42-50

Rapid report | Free Access

The auxin response factor MONOPTEROS controls meristem function and organogenesis in both the shoot and root through the direct regulation of *PIN* genes

Naden T. Krogan, Danielle Marcos, Aaron I. Weiner, Thomas Berleth

First published: 21 July 2016
https://doi.org/10.1111/nph.14107
Citations: 67

Summary

- The regulatory effect auxin has on its own transport is critical in numerous self-organizing plant patterning processes. However, our understanding of the molecular mechanisms linking auxin signal transduction and auxin transport is still fragmentary, and important regulatory genes remain to be identified.
- To track a key link between auxin signaling and auxin transport in development, we established an *Arabidopsis thaliana* genetic background in which fundamental patterning processes in both shoot and root were essentially abolished and the expression of PIN FORMED (PIN) auxin efflux facilitators was dramatically reduced.
- In this background, we demonstrate that activating a steroid-inducible variant of the auxin response factor (ARF) MONOPTEROS (MP) is sufficient to restore patterning and *PIN* gene expression. Further, we show that MP binds to distinct promoter elements of multiple genetically defined *PIN* genes.
- Our work identifies a direct regulatory link between central, well-characterized genes involved in auxin signal transduction and auxin transport. The steroid-

> inducible MP system directly demonstrates the importance of this molecular link in multiple patterning events in embryos, shoots and roots, and provides novel options for interrogating the properties of self-regulated auxin-based patterning *in planta*.

Introduction

All stages of plant growth and development depend critically on the action of the phytohormone auxin. Auxin is required to establish the body plan during embryogenesis and later plays a key role in the initiation and outgrowth of new organs from stem cell regions called apical meristems (Vanneste & Friml, 2009). Many processes in both the shoot apical meristem (SAM) and root apical meristem (RAM) involve auxin distribution patterns. For example, in the shoot, the positioning and growth of new organs are dictated by auxin concentration maxima established by the PIN FORMED (PIN) family of membrane efflux facilitators, which mediate polar auxin transport between cells (Adamowski & Friml, 2015). The canonical auxin signaling pathway, which involves the auxin response factor (ARF) family of transcriptional regulators, is required to elicit the appropriate developmental output in response to these local concentration maxima (Chapman & Estelle, 2009).

Many auxin-dependent patterning events have a self-organizing property consistent with a proposed ability of auxin to regulate and reinforce its own flow (Vanneste & Friml, 2009). In particular, an influence of auxin on the expression and subcellular localization of PIN efflux carriers is a central prerequisite of self-organization in plant patterning according to many mathematical models (Kuhlemeier, 2007). Consistent with this, some *PIN* genes appear to be primary auxin response genes (Vieten *et al*., 2005; Dello Ioio *et al*., 2008; Chen *et al*., 2015). Additionally, auxin can influence PIN subcellular localization to control auxin flow and, in turn, the positioning and growth of new tissues and organs (Benkova *et al*., 2003; Sauer *et al*., 2006).

Whereas modulation of PIN protein localization and stability has been thoroughly analyzed for years, molecular details regarding the direct transcriptional control of *PIN*s are clearly incomplete. Most transcription factors that have been implicated in *PIN* regulation have not been linked to the ARF-mediated canonical auxin signal transduction pathway (Cui *et al*., 2013; Garay-Arroyo *et al*., 2013; Wang *et al*., 2015), but

there are a few recent exceptions. For instance, among a group of cytokinin response factors (CRFs) that target *PIN* genes (Simaskova *et al*., 2015), one (CRF2) is itself regulated by ARF5/MONOPTEROS (MP) (Schlereth *et al*., 2010). Further, ARF7/NONPHOTOTROPIC HYPOCOTYL4 (NPH4) and FOUR LIPS/MYB124 have been shown to jointly and directly target *PIN3* in the root (Chen *et al*., 2015). However, mutations in each of these direct regulators of *PIN*s result in rather subtle defects in specific aspects of root development, suggesting that important molecular links between auxin signaling and auxin transport remain to be identified.

The functions of ARF5/MP and ARF7/NPH4 have been shown to be asymmetrically redundant (Hardtke *et al*., 2004). ARF7/NPH4, a regulator of phototropic auxin responses, has a gratuitous and dispensable function in patterning processes, visible in the *nph4* mutant only through its enhancement of *mp* patterning defects. In the *mp nph4* double mutant, structure and function of both apical meristems are abolished, suggesting a complete collapse in auxin-mediated patterning (Hardtke *et al*., 2004). Importantly, however, such defects are undetectable in *nph4* single mutants, indicating that ARF5/MP is sufficient for all auxin-mediated patterning in both roots and shoots. In this study, we have introduced an inducible variant of *MP*, *MP-GR*, into the *mp nph4* double mutant (Krogan *et al*., 2014). This background demonstrated that MP is sufficient to restart auxin-mediated patterning processes from completely disorganized tissue in both shoots and roots. As such, this establishes a genetic system that can provide insight into auxin-mediated self-organization by revealing the consequences of flexibly restarting patterning processes in diverse developmental stages. Further, we demonstrate that the expression of at least three *PIN* genes is strongly dependent on MP, which activates their transcription by binding to discrete elements in the promoters of each gene. Based on the dramatic phenotypes reported for multiple *arf* as well as multiple *pin* mutant combinations, our results indicate that ARF5/MP functions as a central connector between auxin signal transduction and auxin transport.

Materials and Methods

Plant material and growth conditions

Unless stated otherwise, *Arabidopsis thaliana* (L.) Heynh seeds were plated and plants grown as described (Hardtke *et al*., 2004). Mutant alleles used were *mpG12*, *mpBS1354*

(Hardtke & Berleth, 1998) and *nph4-1* (Harper *et al*., 2000). Transgenic lines *mp nph4 MP-GR* (Krogan *et al*., 2014), *PIN1::PIN1-GFP* (Benkova *et al*., 2003), *MP::MP-GUS* (Vidaurre *et al*., 2007) and *MP::MP-GFP* (Cole *et al*., 2009) have been described previously.

Transgene construction

To make *PIN* transcriptional reporter genes, 2011, 2020 and 2108 bp upstream of the translational start codons of *PIN1*, *PIN3*, and *PIN7*, respectively, were fused to the *β-glucuronidase* (*GUS*) reporter gene and transformed into the Columbia-0 ecotype.

Reverse transcription-polymerase chain reaction (RT-PCR)

cDNA template preparation was performed as previously reported (Krogan *et al*., 2014). For shoot samples, PCR reactions of cDNA template included 1.2 μCi Redivue [α-^{32}P] dCTP (Amersham Biosciences, Mississauga, ON, Canada) to facilitate product quantification. Low cycle numbers (24 cycles) were used to prevent saturation of product amplification. Further, at least two concentrations of template were amplified in parallel to ensure that a doubling of the amount of starting template resulted in a proportional doubling of the final PCR product. Electrophoresed RT-PCR products were scanned by a Personal Molecular Imager FX Scanner and quantified by accompanying Quantity One Quantitation Software (Bio-Rad). Root samples were analyzed similarly, except that radioactive labeling was omitted and product intensity was instead quantified by ImageJ software (National Institutes of Health, Bethesda, MD, USA). Primer sequences are given in Supporting Information Table S1.

Electrophoretic mobility shift assays (EMSAs)

The purification of His-MP(432) protein and EMSA experimental conditions have been described previously (Krogan *et al*., 2014). Labeled probes were created by PCR reactions containing 20 μCi of Redivue [α-^{32}P] dCTP (Amersham Biosciences). Primer sequences are provided in Table S2. The nonspecific competitor used in EMSAs corresponded to –1870 to –1729 bp (relative to translational start) of *PIN3*.

Chromatin immunoprecipitation (ChIP)

Chromatin immunoprecipitation experiments on floral tissue of *MP::MP-GFP* were performed as previously described (Krogan *et al*., 2012). Real-time PCR on ChIP

samples was performed with a Mx3005P QPCR system (Agilent Technologies, Santa Clara, CA, USA) using PerfeCTa SYBR Green SuperMix (Quanta Biosciences Inc., Beverly, MA, USA). Data analysis was carried out using MxPro QPCR software (Agilent Technologies). Enrichment was calculated as a ratio of the signal from ChIP samples to that from input samples. Fold enrichment was calculated as the ratio of *MP::MP-GFP* sample enrichment to nontransgenic control sample enrichment and was normalized using *ACT7* data. Primer sequences are given in Table S3.

Microtechniques and microscopy

For low to medium magnification, samples were viewed under bright field and fluorescence illumination (green fluorescence protein (GFP)) with a Leica MZ FLIII (Leica Microsystems, Wetzlar, Germany) dissecting stereomicroscope. For high magnification, samples were viewed under differential interference contrast (DIC) optics with an Olympus AX70 microscope (Olympus Canada Inc., Richmond Hill, ON, Canada). For confocal laser scanning microscopy of roots, samples were mounted in water or 10 μg ml^{-1} propidium iodide (PI) and observed with a Zeiss Axiovert 100M microscope equipped with a Zeiss LCM510 laser module confocal unit. Analysis of GUS activity was as described in Krogan *et al*. (2014) with modifications (Table S4a,b). ImageJ software was used to create rainbow spectrum look-up-table images of GFP signal intensity and to quantify angles of root tropic growth.

Results and Discussion

To investigate the influence of MP on postembryonic development, we sought to remove redundant contributions of NPH4 to MP-mediated processes by analyzing *mp nph4* expressing an inducible *MP-GR* transgene driven by native *MP* regulatory sequence (Krogan *et al*., 2014). Further, since *mp nph4* embryos fail to produce cotyledons and functional apical meristems (Hardtke *et al*., 2004) in some experiments we bypassed embryonic abnormalities by continually providing *mp nph4 MP-GR* parental plants with the synthetic glucocorticoid dexamethasone (DEX), which activates MP-GR function. This restored embryo patterning in seeds and led to the germination of seedlings with rescued apical–basal axis formation (Fig. 1a), but was followed by rapid deterioration of postembryonic development in the absence of DEX. In the following, we use this background as a genetic switch to restart auxin-driven

patterning in individuals after either impaired or normalized embryogenesis and refer to these as *mp nph4 MP-GR* or *mp nph4 MP-GR*^{er} (embryonically rescued), respectively.

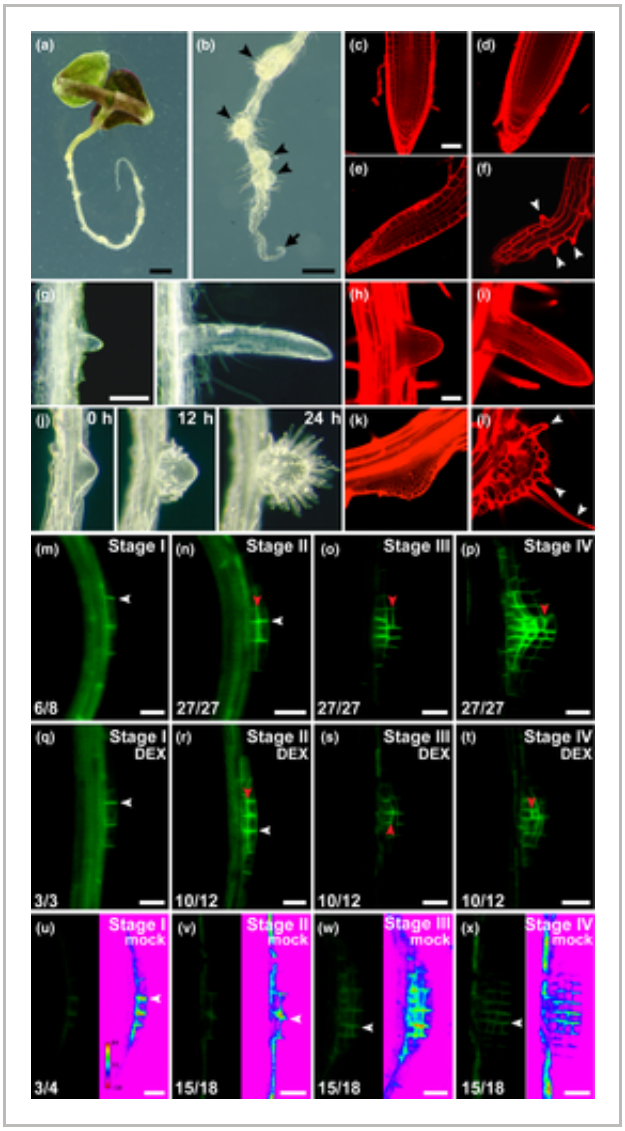

Figure 1

Open in figure viewer | PowerPoint

The role of MONOPTEROS (MP) in root apical meristem (RAM) maintenance and lateral root patterning in *Arabidopsis*. (a, b) At 9 d after germination (DAG) *mp nph4 MP-GR*^{er} seedlings grown in the absence of dexamethasone (DEX). Disorganized lateral roots (arrowheads) and inactive primary root tip (arrow) are indicated. (c–f) Confocal images of primary roots. (c, d) *mp nph4 MP-GR*^{er} grown on 15 μM DEX at 4 DAG (c); RAM is normal and resembles *nph4* root at 4 DAG (d). (e, f) *mp nph4 MP-GR*^{er} RAMs grown in the absence of DEX at 4 DAG (e) and 6 DAG (f). Arrowheads indicate epidermal root hair cells. (g) Lateral roots from *mp nph4 MP-GR*^{er}

seedlings grown on 15 μM DEX. (h, i) Confocal images of *nph4* lateral roots showing normal RAM. (j–l) Time course (j) and confocal images (k, l) of lateral root primordia (LRPs) from *mp nph4 MP-GR*^{er} seedlings grown in the absence of DEX. Arrowheads denote root hairs. (m–x) PIN1-GFP in LRPs (distal tip to the right). (m–p) Wild-type. (q–x) *mp nph4 MP-GR*^{er} germinated and grown continuously with (q–t) or without (u–x) 15 μM DEX. Transverse and lateral cell membranes are denoted by white and red arrowheads, respectively. Ratios of LRPs exhibiting the depicted PIN1-GFP distribution and intensity are shown. LRPs in (u–x) are also depicted as rainbow spectrum look-up-tables to show relative PIN1-GFP expression. LRP stages are according to Malamy & Benfey (1997). Bars: (a) 1 mm; (b) 0.5 mm; (c–f, h, i, k, l) 50 μm; (g, j) 0.2 mm; (m–x) 20 μm.

Role of MP in RAM function

The formation of a primary RAM and positions of new lateral root primordia (LRPs) are dictated by local auxin response maxima (Sabitini *et al*., 1999; Benkova *et al*., 2003). The *mp nph4 MP-GR*^{er} phenotype demonstrates the critical impact of MP regulatory potential on postembryonic *de novo* root organization and on maintenance of the RAM, which would not have been evident in *mp* single mutants (Fig. S1a,b). In untreated *mp nph4 MP-GR*^{er} primary roots, initial elongation is invariably followed by growth cessation after 4 d postgermination (Figs 1a,b, S2a). This is accompanied by the gradual disintegration of the RAM, as cell file numbers decrease and terminal differentiation occurs, evidenced by increased cell size and root hair production close to the root tip (Fig. 1e,f). Conversely, continuous DEX treatment maintains normal RAM organization and function (Fig. 1c). Furthermore, DEX exposure establishes a concentration-dependent memory effect, as duration of *mp nph4 MP-GR*^{er} root growth in the absence of DEX directly correlates with the extent of prior treatment (Fig. S2a). Our findings also implicate MP activity in gravitropic responses, as untreated *mp nph4 MP-GR*^{er} roots are agravitropic, a defect that can be rescued by DEX application (Fig. S1c).

ARF19 and *ARF7*/*NPH4* have been shown to act redundantly in the initiation of LRPs (Okishuma *et al*., 2005), a developmental process that is retained in *mp nph4 MP-GR*^{er} seedlings. Under continuous DEX exposure, *mp nph4 MP-GR*^{er} lateral roots exhibit proper patterning and outgrowth similar to *nph4* mutants (Fig. 1g–i). By contrast, lateral organs of untreated *mp nph4 MP-GR*^{er} roots display gross morphological abnormalities not previously seen in other mutant backgrounds (Fig. 1b,j), apparently reflecting MP function in LRP development (De Smet *et al*., 2010). Initially, an increased

number of cells are recruited into LRPs of these mutants, resulting in broader outgrowths (Fig. 1j,k). Upon further development, the excessively wide primordia fail to specify distal cell identities and hence a functional RAM. Instead, these cell masses typically arrest and become covered with epidermal root hair cells, suggesting that they comprise only unspecified or proximal cell identities and fail to maintain a stem cell niche (Fig. 1j,l).

Aspects of root growth affected in untreated *mp nph4 MP-GR*^{er} seedlings are reminiscent of roots compromised in PIN-mediated auxin transport, including an inability to pattern and maintain a RAM, agravitropism and widened LRPs (Geldner *et al*., 2001, 2004; Benkova *et al*., 2003). Therefore, we investigated whether *PIN1::PIN1-GFP* expression is altered in *mp nph4 MP-GR*^{er}. In wild-type and DEX-treated *mp nph4 MP-GR*^{er}, PIN1-GFP localizes to the transverse sides of LRP initial cells (Fig. 1m,q). Subsequent LRP development is characterized by a prominent shift in PIN1-GFP localization to lateral sides of cells (Fig. 1n–p,r–t), which is associated with the focusing of auxin transport to the tip of growing primordia (Benkova *et al*., 2003). In LRPs of untreated *mp nph4 MP-GR*^{er} roots, intensity of PIN1-GFP expression was dramatically reduced in all stages, while prominent relocalization of PIN1 to lateral sides of cells was not apparent (Fig. 1u–x). This suggests that abnormalities in LRP patterning in *mp nph4* are the result of defects in both the expression and subcellular relocalization of PIN1.

We sought to determine whether reactivation of MP in *mp nph4 MP-GR*^{er} roots was sufficient to restore PIN1-GFP levels and to rescue RAM patterning and function. Upon transfer of *mp nph4 MP-GR*^{er} seedlings to DEX media, almost half of early LRPs analyzed showed an extremely rapid increase in PIN1-GFP levels and exhibited correct relocalization of PIN1 to lateral cell surfaces (Fig. 2d–f). By contrast, PIN1-GFP in wild-type roots treated with DEX showed no change or a decrease in expression level, while subcellular localization remained normal (Fig. 2a–c). Strikingly, when older LRPs from untreated *mp nph4 MP-GR*^{er} seedlings were transferred to DEX, lateral roots with normalized RAMs emerged from within the disorganized cell masses (Fig. 2g–i). This *de novo* RAM emergence was associated with the initiation of PIN1-GFP expression foci within the interior cells (Fig. 2j). These results implicate PIN1 as a major target of MP in the control of root patterning. Finally, the primary roots of older untreated *mp nph4 MP-GR*^{er} seedlings were incapable of reinitiating growth upon transfer to DEX

(Fig. 2g,h), possibly because of the absence of reversible cell states among the very few cells in these locations (Fig. 1f).

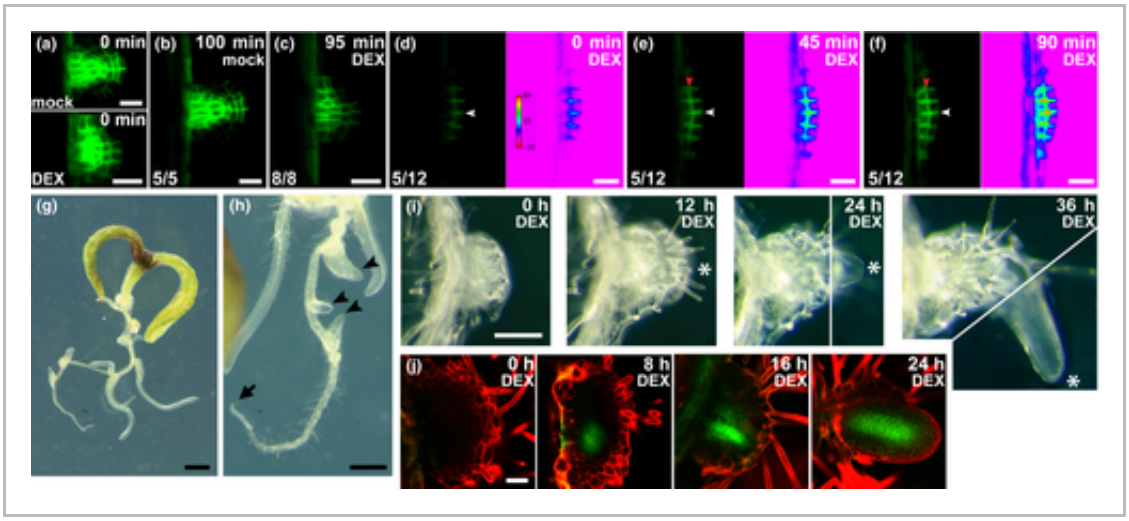

Figure 2

Open in figure viewer | PowerPoint

Effect of MONOPTEROS (MP) on lateral root normalization and PIN FORMED1 (PIN1) activation in *Arabidopsis*. (a–f) PIN1-GFP in lateral root primordia (LRPs) of seedlings (distal tip to the right) at 4–5 d after germination (DAG). (a–f) Wild-type (a–c) and *mp nph4 MP-GR*^{er} (d–f) LRPs (with rainbow spectrum look-up-tables) transferred to 15 µM dexamethasone (DEX) at 0 min. Ratios of LRPs exhibiting the depicted PIN1-GFP distribution and intensity are shown. LRPs that differed from images depicted in (d–f) did not show an increase in PIN1-GFP expression. Transverse and lateral cell membranes are denoted by white and red arrowheads, respectively. (g, h) Seedlings at 9 DAG germinated and grown without DEX for 6 d, then transferred to 15 µM DEX for 3 d. When transferred at 6 DAG, the primary root tip (arrow) had ceased growth and disorganized lateral outgrowths had initiated. Arrowheads point to emerging lateral roots. (i) Time course of *mp nph4 MP-GR*^{er} lateral root outgrowth transferred to 30 µM DEX at 0 h. Asterisks denote an emerging lateral root. The 24 and 36 h pictures are composites of two images (separated by white lines) at different focal planes. (j) PIN1-GFP expression in *mp nph4 MP-GR*^{er} lateral root outgrowths of 8 DAG seedlings transferred to 30 µM DEX at 0 h. Bars: (a–f) 20 µm; (g) 1 mm; (h) 0.5 mm; (i) 0.2 mm; (j) 50 µm.

Role of MP in SAM function

The initiation sites of shoot lateral organs are defined by areas of high PIN1

expression (with PIN1 protein localization suggestive of auxin transport towards convergence points), and in mathematical models of organ positioning, auxin signal transduction and transport constitute key parameters (Sassi & Vernoux, 2013). Consistent with this, both *mp* and *pin1* mutants display severe distortions in this positioning process (Okada *et al*., 1991; Przemeck *et al*., 1996), and *mp nph4* double mutants fail to form such organs at all (Hardtke *et al*., 2004). By controllably activating MP in *mp nph4 MP-GR*^{er} seedlings, we observed that continuous MP activity was required for shoot organ formation, and that the intensity and duration of MP induction correlated with the extent of organ production (Fig. S2b). These findings reveal the sensitivity of the self-organizing patterning process, which appears continuously reliant on MP activity.

In the absence of MP and NPH4 activity, SAMs do not show signs of lateral organ outgrowth for 2–3 wk (Fig. 3a,b,l,o), after which they generate lateral bulges that vary in their spatial arrangement depending on whether cotyledons are present (Fig. 3c–f). If cotyledons are absent (as in *mp nph4* MP-GR), the primary SAM turns into a rotationally symmetrical, grossly oversized apical mound (Fig. 3a,b) that goes on to initiate lateral bulges evenly spaced over its entire surface (Fig. 3c,d). By contrast, if cotyledons are present (as in *mp nph4 MP-GR*^{er}), SAMs become more elliptical in shape (Fig. 3l,o) and later initiate equally spaced bulges along a straight line perpendicular to the axis connecting the cotyledons (Fig. 3e,f). These findings suggest that under conditions of highly diminished ARF activity, position-defining auxin focusing, as described for normal SAMs (Sassi & Vernoux, 2013), is extremely delayed but qualitatively unchanged. In the absence of cotyledons, the previously postulated auxin-based lateral inhibition model (Reinhardt *et al*., 2003) would predict new initiation positions to be largely random but separated as far as possible from one other (Fig. 3c,d). In the presence of cotyledons, the same principles, in combination with the postulated inhibitory influence of cotyledons, would also be consistent with the observed distribution of primordia (Fig. 3e,f).

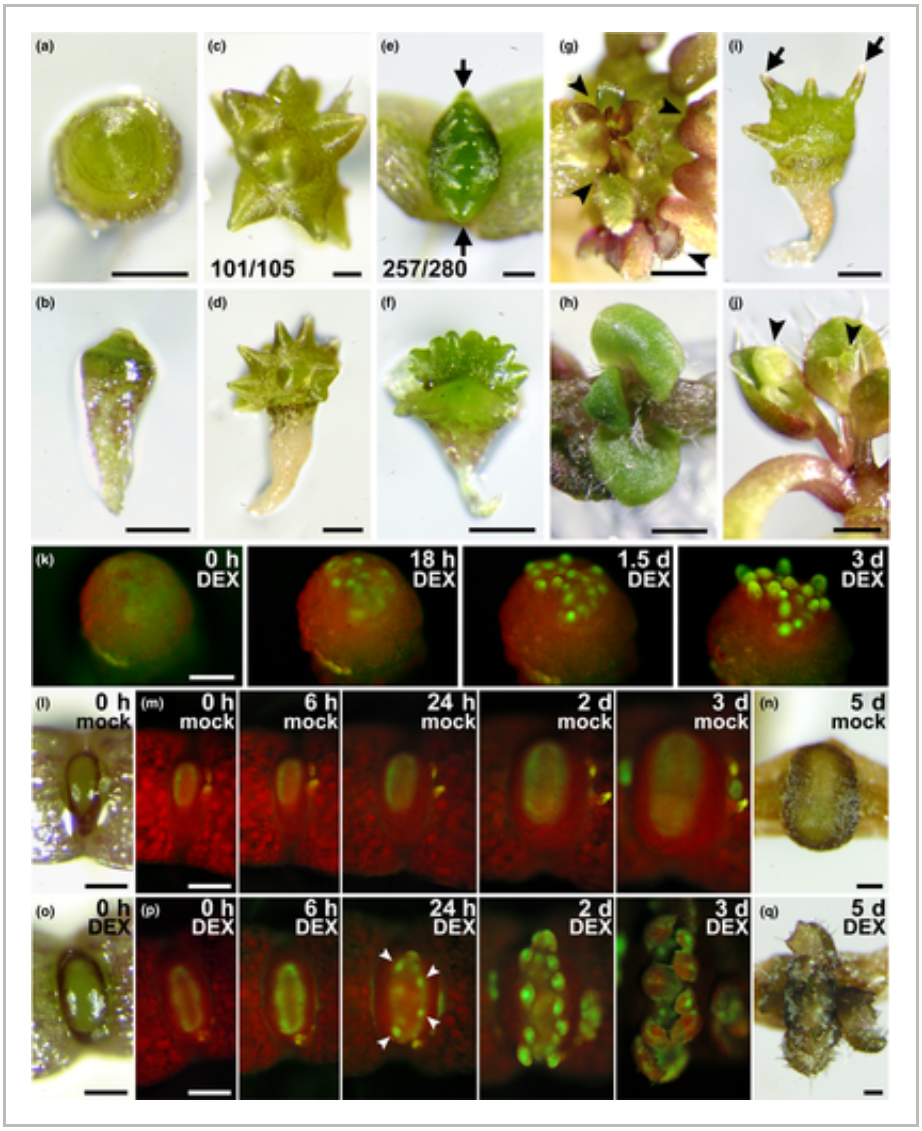

Figure 3

Open in figure viewer | PowerPoint

Effect of MONOPTEROS (MP) activity on shoot organ initiation and PIN FORMED1 (PIN1) expression in *Arabidopsis*. (a, b) Apical (a) and lateral views (b) at 17 d after germination (DAG) of *mp nph4 MP-GR* seedlings grown in the absence of dexamethasone (DEX). (c–f) Apical and lateral views of *mp nph4 MP-GR* (c, d) and *mp nph4 MP-GR*^{er} (e, f) seedlings (24 DAG) grown in the absence of DEX. The fractions of *mp nph4 MP-GR* individuals with randomly arranged lateral bulges (c) and of *mp nph4 MP-GR*^{er} seedlings with lateral bulges arranged in a linear plane perpendicular to cotyledons (arrows, e) are given. Cotyledons have been removed in (f) to allow visualization of bulges. (g) Clusters of leaf-like organs (arrowheads) initiated from lateral bulges of *mp nph4 MP-GR* seedlings transferred to 15 µM DEX at 17 DAG and grown for an additional 11 d. (h) Apical view at 17 DAG of

mp nph4 MP-GR^{er} seedling transferred to 15 μM DEX at 10 DAG. (i) *mp nph4 MP-GR* seedling (28 DAG) grown in the absence of DEX. Lateral bulges have transitioned to tapered, pin-like structures (arrows). (j) Flowers (arrowheads) initiated from pin-like shoot apical meristem (SAM) outgrowths of 28 DAG *mp nph4 MP-GR* seedlings transferred to 15 μM DEX at 17 DAG. (k) PIN1-GFP expression in the SAM of an *mp nph4 MP-GR* seedling (13 DAG) lacking cotyledons, transferred to 30 μM DEX at 0 h. Foci of PIN1-GFP expression at 18 h presage lateral organ positions. (l–q) PIN1-GFP expression in dicotyledonous *mp nph4 MP-GR*^{er} seedlings (10 DAG) transferred to mock (l–n) or 30 μM DEX (o–q) at 0 h. Appearances of the SAMs at the start (l, o) and end (n, q) of each time course are shown. A uniform ring of PIN1-GFP shows increased expression by 6 h of DEX treatment (p). PIN1-GFP foci (arrowheads at 24 h) presage lateral organ formation. Bars: (a, b, d, f, g, i, j) 0.5 mm; (c, e) 0.2 mm; (h) 1 mm; (k–q) 0.2 mm.

The lateral bulges formed in the absence of DEX are meristematic in identity, as transfer to DEX shortly after their formation results in each bulge initiating an array of leaf-shaped organs (Fig. 3g). The ability of MP to promote leaf formation is also reflected in the immediate generation of leaves (as opposed to later-forming bulges) in *mp nph4 MP-GR* and *mp nph4 MP-GR*^{er} primary SAMs treated with DEX shortly after germination (Fig. 3h). By contrast, if the bulges develop in the continued absence of DEX, they enter reproductive growth as evidenced by their transition into pin-like inflorescence stems (Fig. 3i), which initiate flowers when finally exposed to DEX (Fig. 3j). These findings indicate that MP is continuously required for the formation of leaves but has no influence on the transition to reproductive development.

Because PIN1 is postulated to have an instrumental role in primordia initiation and positioning in the SAM (Benkova *et al*., 2003; Reinhardt *et al*., 2003), abnormalities displayed by *mp nph4* SAMs may be the result of reduced PIN1 expression. Visualization of PIN1-GFP supports this interpretation, as PIN1 expression in SAMs of *mp nph4 MP-GR* seedlings (which lack cotyledons) is not apparent even after 2 wk postgermination (Fig. 3k, left). Expression of PIN1-GFP is only faintly visible in dicotyledonous *mp nph4 MP-GR*^{er} seedlings, where it forms a stable ring of homogeneous intensity in the peripheral zone of the narrow, oval SAM (Fig. 3m,p). The effect of MP-GR activation on PIN1 expression in both seedling types is immediate and dramatic. Upon DEX application to *mp nph4* MP-GR SAMs, distinct spots of strong PIN1-GFP expression become visible within 18 h, then further intensify to eventually become associated with outgrowing primordia (Fig. 3k). In *mp nph4 MP-GR*^{er} SAMs, DEX

application increases ring-shaped PIN1 expression after 6 h (Fig. 3p). Together with increased intensity, PIN1-GFP expression becomes uneven by 24 h, narrowing into bright foci that precede organ primordia. As the SAM grows for the next 2 d, more PIN1 expression foci emerge, which also mark organ initiation sites (Fig. 3p).

In summary, our analysis of the SAM identifies ARF activity as the transcriptional driving force underlying dynamic PIN1 expression, auxin distribution and eventually organ initiation and phyllotaxis. In the near-absence of ARF activity, the generation of PIN1 expression foci and lateral organs is strongly attenuated and shoot development operates in vastly different dimensions and timescales. Intriguingly, MP remains sufficient to restore organ production from these abnormal conditions. As a genetic tool, this ability of a single gene to controllably reset the self-organizing process of organ initiation under various experimentally designed conditions, including those with or without positional references, affords a tremendous opportunity to interrogate the underlying principles and mechanisms of auxin-based patterning.

Direct regulation of *PIN* genes by MP

The rapid response of PIN1-GFP expression levels to MP activity (Figs 2d–f, 3p) suggests direct regulation of *PIN1* by MP. To test this, we quantified *PIN1* transcript abundance by RT-PCR on isolated *mp nph4 MP-GR*^{er} roots and shoots treated with varying combinations of DEX, auxin and the translational inhibitor cycloheximide (Fig. 4a,b). In cycloheximide-treated root tissue, DEX-mediated MP activation resulted in over fivefold induction of *PIN1* expression in the presence of auxin (Fig. 4a). We further monitored expression of *PIN3* and *PIN7* and found both to be responsive to MP activity under conditions of translational inhibition (Fig. 4a). In auxin-treated *mp nph4 MP-GR*^{er} SAMs, all three tested *PIN* genes were also reproducibly up-regulated by MP activation in the presence of cycloheximide (Fig. 4b). Consistent with these observations, *PIN1*, *PIN3* and *PIN7* show auxin-inducible expression (Fig. S3a) (Vieten *et al*., 2005) and have been implicated in RAM patterning (Blilou *et al*., 2005). Furthermore, the spatiotemporal expression profiles of all three *PIN* genes show significant overlap with MP in a variety of developmental contexts (Fig. S3b). Collectively, these results indicate that *PIN1*, *PIN3* and *PIN7* are direct transcriptional targets of MP.

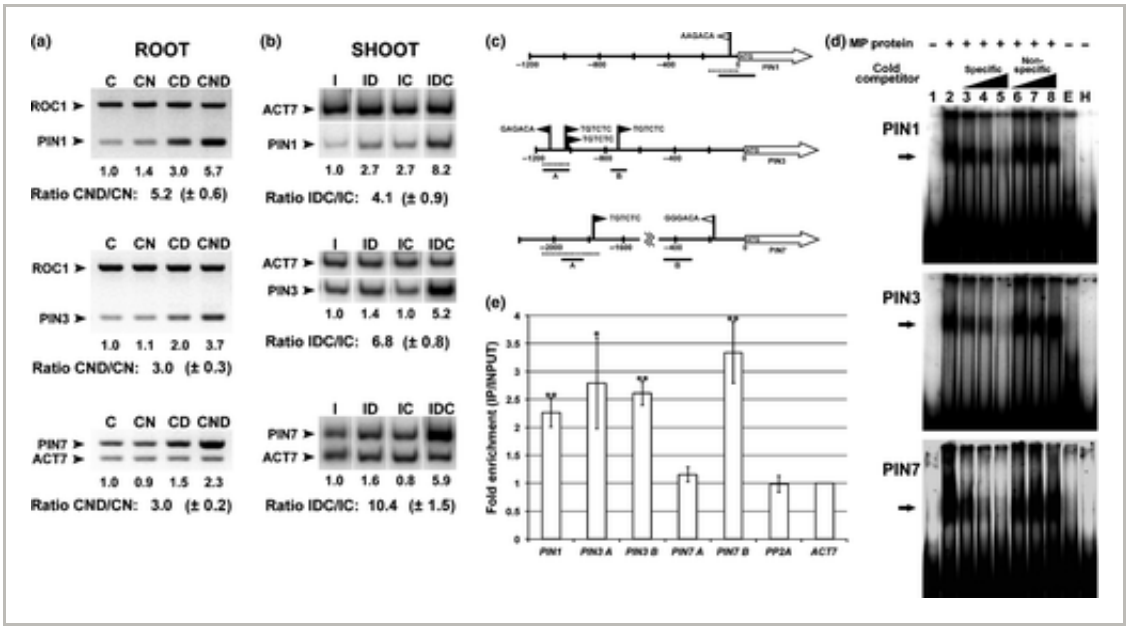

Figure 4

Open in figure viewer | PowerPoint

Binding of MONOPTEROS (MP) to *PIN FORMED* (*PIN*) upstream regulatory regions. (a) Reverse transcription-polymerase chain reaction (RT-PCR) on dissected *mp nph4 MP-GR*^{er} roots (8–9 d after germination (DAG)) treated for 4 h with 30 μM cycloheximide (C) and varying combinations of 5 μM α-naphthaleneacetic acid (N) and 30 μM dexamethasone (D). *ROC1* or *ACT7* genes are internal controls used for normalization. Normalized signal in lane (C) was arbitrarily set to 1.0. Mean ± SEM of the normalized CND/CN ratios for three independent biological replicates are given. (b) RT-PCR on dissected *mp nph4 MP-GR*^{er} shoot apical meristems (SAMs) (21 DAG) treated for 4 h with 10 μM indole-3-acetic acid (I) and varying combinations of 30 μM dexamethasone (D) and 30 μM cycloheximide (C). *ACT7* is an internal control used for normalization. Normalized signal in lane (I) was arbitrarily set to 1.0. Mean ± SEM of the normalized IDC/IC ratios for three independent biological replicates are given. (c) Schematics of *PIN* promoters. Arrows depict open reading frames (ORFs), black flags mark consensus auxin response elements (AuxREs), and white flags denote near-perfect AuxREs. Dashed bars designate regions used as electrophoretic mobility shift assay (EMSA) probes in (d), while solid bars delineate regions tested by chromatin immunoprecipitation (ChIP) PCR in (e). (d) EMSAs using *PIN* DNA probes and recombinant His-MP(432) protein. Arrows indicate positions of MP–probe complexes. Lanes 3–5 and lanes 6–8 contain increasing amounts (10× , 50× , 100×) of specific unlabeled competitor DNA and nonspecific unlabeled DNA lacking consensus AuxREs, respectively. Lane E contains protein from an empty vector control purification. Lane H contains an unrelated prokaryotic protein with the same amino-terminal His-tag as the MP protein. (e) Anti-GFP

ChIP of *MP::MP-GFP* tissue showing fold enrichment of *PIN* promoter regions depicted in (c). Mean fold enrichments ± SEM for three independent biological replicates are shown. Student's *t*-test was used to determine the significance of target enrichment relative to enrichment of *PP2A* control (*, $P < 0.05$; **, $P < 0.01$).

To delineate which *PIN cis*-regulatory regions are directly targeted by MP, we performed *in vitro* and *in vivo* binding assays on *PIN1*, *PIN3* and *PIN7* promoters, each of which contain canonical or near-canonical auxin response elements (AuxREs) (Fig. 4c). MP specifically bound AuxRE-containing promoter fragments of all three tested *PIN*s in EMSAs (Fig. 4d). ChIP was performed on *MP::MP-GFP* to test these interactions *in planta*, and, at least for *PIN1* and *PIN3*, MP bound the same promoter regions identified by EMSA (Fig. 4e). Interestingly, this tested region of *PIN3* was recently identified as a binding site for ARF7, and the mutation of its three canonical AuxREs reduces the auxin inducibility of *PIN3* (Chen *et al*., 2015). Downstream of this region, another canonical AuxRE exists (Fig. 4c), the position of which also showed enrichment in MP ChIP analyses (Fig. 4e). In the case of *PIN7*, ChIP did not show enrichment of the promoter fragment bound by MP *in vitro* (Fig. 4e). We therefore scanned the *PIN7* promoter for near-consensus AuxREs and found one such element at a more proximal position (Fig. 4c). Our *MP::MP-GFP* ChIP analysis showed enrichment in the vicinity of this proximal position (Fig. 4e). Together, our results demonstrate that MP binds to AuxRE-containing regulatory regions in the promoters of *PIN1*, *3* and *7 in planta*, and that through this binding, MP is strictly required for RAM maintenance, LRP patterning and SAM lateral organ initiation.

A central molecular link between auxin signaling and auxin transport

Like other key processes in plant development, the formation of new organs in roots and shoots has been attributed to the dynamic, self-organizing interplay between auxin signal transduction and auxin transport. The regulatory relationships between critical parameters of this interplay have remained subject to mathematical modeling (Kuhlemeier, 2007), and many of the corresponding cellular mechanisms have yet to be unravelled. Surprisingly, however, one central tenet in most mathematical models, a positive regulation of auxin transport by auxin, has not been adequately explained at the molecular level. In most models, disruption of this regulation should have the most dramatic consequences on respective patterning processes (Wabnik *et al*., 2013),

but hitherto no genes with correspondingly severe mutant phenotypes have been implicated. In this study, we have demonstrated that *mp*, in an appropriate multiple mutant background, displays the severe patterning defects expected for a critical connector between auxin and auxin transport. In this capacity, MP serves as a nearly perfect on–off switch regulating *PIN* expression and organ formation in both roots and shoots. This regulation occurs through direct binding of MP to distinct promoter elements in multiple *PIN* genes, and the possibility of controlling the entire process through the nuclear entry of a single transcription factor provides vast opportunities to interrogate the systems properties of auxin's self-organizing regulation.

Acknowledgements

We would like to thank our colleagues J. Friml and D. Weijers for *PIN1::PIN1-GFP* and *MP::MP-GFP Arabidopsis* seeds, respectively. This work was supported by a Natural Sciences and Engineering Research Council of Canada discovery grant to T.B. as well as support from the Center for Analysis of Genome Evolution and Function (CAGEF). Research reported in this publication was also supported by the National Institute of General Medical Sciences of the National Institutes of Health under award number R15GM114733 to N.T.K. The content is solely the responsibility of the authors and does not necessarily represent the official views of the National Institutes of Health.

Author contributions

N.T.K. and T.B. planned and designed the research and wrote the manuscript. N.T.K., D.M. and A.I.W. performed the experiments.

Please note: Wiley Blackwell are not responsible for the content or functionality of any Supporting Information supplied by the authors. Any queries (other than missing material) should be directed to the *New Phytologist* Central Office.

Filename	Description
nph14107-sup-0001-SupInfo.pdf PDF document, 541 KB	**Fig. S1** *Arabidopsis* root gravitropic responses. **Fig. S2** *mp nph4 MP-GR*^{er} root and shoot apical meristem activity depends directly on dexamethasone (DEX) dosage in *Arabidopsis*. **Fig. S3** *Arabidopsis PIN FORMED* (*PIN*)::*β-glucuronidase* (*GUS*) expression patterns. **Table S1** Reverse transcription-polymerase chain reaction **(**RT-PCR) primer sequences **Table S2** Primer sequences used to create electrophoretic mobility shift assay (EMSA) probes **Table S3** Chromatin immunoprecipitation (ChIP) primer sequences **Table S4** β-Glucuronidase (GUS)-staining conditions of auxin-induced *Arabidopsis* tissues; GUS-staining conditions of *Arabidopsis* tissues that were not auxin-treated

Please note: The publisher is not responsible for the content or functionality of any supporting information supplied by the authors. Any queries (other than missing content) should be directed to the corresponding author for the article.

Adamowski M, Friml J. 2015. PIN-dependent auxin transport: action, regulation, and evolution. *Plant Cell* **27**: 20–32.

CAS | PubMed | Web of Science® | Google Scholar

Benkova E, Michniewicz M, Sauer M, Teichmann T, Seifertova D, Jurgens G, Friml F. 2003. Local, efflux-dependent auxin gradients as a common module for plant organ formation. *Cell* **115**: 591–602.

CAS | PubMed | Web of Science® | Google Scholar

Blilou I, Xu J, Wildwater M, Willemsen V, Paponov I, Friml J, Heidstra R, Aida M, Palme K, Scheres B. 2005. The PIN auxin efflux facilitator network controls growth and patterning in *Arabidopsis* roots. *Nature* **433**: 39–44.

CAS | PubMed | Web of Science® | Google Scholar

Chapman E, Estelle M. 2009. Mechanism of auxin-regulated gene expression in plants. *Annual Review of Genetics* **43**: 265–285.

CAS | PubMed | Web of Science® | Google Scholar

Chen Q, Liu Y, Maere S, Lee E, Van Isterdael G, Xie Z, Xuan W, Lucas J, Vassileva V, Kitakura S *et al*. 2015. A coherent feed-forward motif model for mediating auxin-sensitive *PIN3* expression during lateral root development. *Nature Communications* **6**: 8821.

CAS | PubMed | Web of Science® | Google Scholar

Cole M, Chandler J, Weijers D, Jacobs B, Comelli P, Werr W. 2009. *DORNROSCHEN* is a direct target of the auxin response factor MONOPTEROS in the *Arabidopsis* embryo. *Development* **136**: 1643–1651.

CAS | PubMed | Web of Science® | Google Scholar

Cui D, Zhao J, Jing Y, Fan M, Liu J, Wang Z, Xin W, Hu Y. 2013. The *Arabidopsis* IDD14, IDD15, and IDD16 cooperatively regulate lateral organ morphogenesis and gravitropism by promoting auxin biosynthesis and transport. *PLoS Genetics* **9**: e1003759.

CAS | PubMed | Web of Science® | Google Scholar

De Smet I, Lau S, Voss U, Vanneste S, Benjamins R, Rademacher EH, Schlereth A, De Rybel B, Vassileva V, Grunewald W *et al*. 2010. Bimodular auxin response controls organogenesis in *Arabidopsis*. *Proceedings of the National Academy of Sciences, USA* **107**: 2705–2710.

CAS | PubMed | Web of Science® | Google Scholar

Dello Ioio R, Nakamura K, Moubayidin L, Perilli S, Taniguchi M, Morita MT, Aoyama T, Costantino P, Sabatini S. 2008. A genetic framework for the control of cell division and differentiation in the root meristem. *Science* **322**: 1380–1384.

 CAS | PubMed | Web of Science® | Google Scholar

Garay-Arroyo A, Ortiz-Moreno E, de la Paz Sánchez M, Murphy AS, García-Ponce B, Marsch-Martínez N, de Folter S, Corvera-Poiré A, Jaimes-Miranda F, Pacheco-Escobedo MA *et al*. 2013. The MADS transcription factor XAL2/AGL14 modulates auxin transport during Arabidopsis root development by regulating PIN expression. *EMBO Journal* **32**: 2884–2895.

 CAS | PubMed | Web of Science® | Google Scholar

Geldner N, Friml J, Stierhof YD, Jurgens G, Palme K. 2001. Auxin transport inhibitors block PIN1 cycling and vesicle trafficking. *Nature* **413**: 425–428.

 CAS | PubMed | Web of Science® | Google Scholar

Geldner N, Richter S, Vieten A, Marquardt S, Torres-Ruiz RA, Mayer U, Jurgens G. 2004. Partial loss-of-function alleles reveal a role for *GNOM* in auxin transport-related, post-embryonic development of *Arabidopsis*. *Development* **131**: 389–400.

 CAS | PubMed | Web of Science® | Google Scholar

Hardtke CS, Berleth T. 1998. The *Arabidopsis* gene *MONOPTEROS* encodes a transcription factor mediating embryo axis formation and vascular development. *EMBO Journal* **17**: 1404–1411.

 Web of Science® | Google Scholar

Hardtke CS, Ckurshumova W, Vidaurre DP, Singh SA, Stamatiou G, Tiwari SB, Hagen G, Guilfoyle TJ, Berleth T. 2004. Overlapping and non-redundant functions of the *Arabidopsis* auxin response factors *MONOPTEROS* and *NONPHOTOTROPIC HYPOCOTYL 4*. *Development* **131**: 1089–1100.

 CAS | PubMed | Web of Science® | Google Scholar

Harper RM, Stowe-Evans EL, Luesse DR, Muto H, Tatematsu K, Watahiki MK, Yamamoto K, Liscum E. 2000. The *NPH4* locus encodes the Auxin Response Factor ARF7, a conditional regulator of differential growth in aerial *Arabidopsis* tissue. *Plant Cell* **12**: 757–770.

 | CAS | PubMed | Web of Science® | Google Scholar

Krogan NT, Hogan K, Long JA. 2012. APETALA2 negatively regulates multiple floral organ identity genes in *Arabidopsis* by recruiting the co-repressor TOPLESS and the histone deacetylase HDA19. *Development* **139**: 4180–4190.

 | CAS | PubMed | Web of Science® | Goo

Krogan NT, Yin X, Ckurshumova W, Berleth T. 2014. Dis
direct targets of ARF5/MP transcriptional regulation. *Ne*

 | CAS | PubMed | Web of Science® | Goo

Kuhlemeier C. 2007. Phyllotaxis. *Trends in Plant Science*

 | CAS | PubMed | Web of Science® | Goo

Malamy JE, Benfey PN. 1997. Organization and cell diffe
Arabidopsis thaliana. *Development* **124**: 33–44.

 | CAS | PubMed | Web of Science® | Goo

Okada K, Ueda J, Komaki MK, Bell CJ, Shimura Y. 1991. F
transport system in early stages of *Arabidopsis* floral bu

 | CAS | PubMed | Web of Science® | Goo

Okishuma Y, Overvoorde PJ, Arima K, Alonso JM, Chan A
Nguyen D *et al*. 2005. Functional genomic analysis of th
members in *Arabidopsis thaliana*: unique and overlappi
Cell **17**: 444–463.

Back

CAS | PubMed | Web of Science® | Go

Przemeck GK, Mattsson J, Hardtke CS, Sung ZR, Berleth
Arabidopsis gene *MONOPTEROS* in vascular developmen
229–237.

CAS | PubMed | Web of Science® | Go

Reinhardt D, Pesce ER, Stieger P, Mandel T, Baltensperg
Kuhlemeier C. 2003. Regulation of phyllotaxis by polar

CAS | PubMed | Web of Science® | Go

Sabitini S, Beis D, Wolkenfelt H, Murfett J, Guilfoyle T, M
N, Weisbeek P *et al*. 1999. An auxin-dependent distal or
Arabidopsis root. *Cell* **99**: 463–472.

PubMed | Web of Science® | Google S

Sassi M, Vernoux T. 2013. Auxin and self-organization a
Experimental Botany **64**: 2579–2592.

CAS | PubMed | Web of Science® | Go

Sauer M, Balla J, Luschnig C, Wisniewska J, Reinohl V, Fr
auxin flow by Aux/IAA-ARF-dependent feedback regula
Development **20**: 2902–2911.

CAS | PubMed | Web of Science® | Go

Schlereth A, Moller B, Liu W, Kientz M, Flipse J, Rademacher EH, Schmid M, Jürgens G, Weijers D. 2010. MONOPTEROS controls embryonic root initiation by regulating a mobile transcription factor. *Nature* **464**: 913–916.

CAS | PubMed | Web of Science® | Google Scholar

Simaskova M, O'Brien JA, Khan M, Van Noorden G, Otvos K, Vieten A, De Clercq I, Van Haperen JM, Cuesta C, Hoyerova K *et al*. 2015. Cytokinin response factors regulate PIN-FORMED auxin transporters. *Nature Communications* **6**: 8717.

 | CAS | PubMed | Web of Science® | Google Scholar

Vanneste S, Friml J. 2009. Auxin: a trigger for change in plant development. *Cell* **136**: 1005–1016.

 | CAS | PubMed | Web of Science® | Google Scholar

Vidaurre DP, Ploense S, Krogan NT, Berleth T. 2007. *AMP1* and *MP* antagonistically regulate embryo and meristem development in *Arabidopsis*. *Development* **134**: 2561–2567.

 | CAS | PubMed | Web of Science® | Google Scholar

Vieten A, Vanneste S, Wiśniewska J, Benková E, Benjamins R, Beeckman T, Luschnig C, Friml J. 2005. Functional redundancy of PIN proteins is accompanied by auxin-dependent cross-regulation of PIN expression. *Development* **132**: 4521–4531.

 | CAS | PubMed | Web of Science® | Google Scholar

Wabnik K, Robert HS, Smith RS, Friml J. 2013. Modeling framework for the establishment of the apical-basal embryonic axis in plants. *Current Biology* **23**: 2513–2518.

 | CAS | PubMed | Web of Science® | Google Scholar

Wang HZ, Yang KZ, Zou JJ, Zhu LL, Xie ZD, Morita MT, Tasaka M, Friml J, Grotewold E, Beeckman T *et al*. 2015. Transcriptional regulation of *PIN* genes by FOUR LIPS and MYB88 during *Arabidopsis* root gravitropism. *Nature Communications* **6**: 8822.

 | CAS | PubMed | Web of Science® | Google Scholar

Citation Statements beta ⓘ

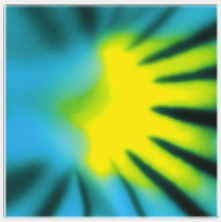

New Phytologist Foundation



OPPORTUNITIES

Subscription Agents
Advertisers & Corporate Partners

CONNECT WITH WILEY

The Wiley Network
Wiley Press Room

WILEY